

Transport Control in Low-Dimensional Spin-1/2 Heisenberg Systems

Lea F. Santos*

Department of Physics, Yeshiva University, 245 Lexington Ave, New York, NY, 10016, USA

(Dated: November 1, 2018)

We analyze transport of local magnetization and develop schemes to control transport behavior in finite spin-1/2 Heisenberg chains and spin-1/2 Heisenberg two-leg ladders at zero temperature. By adjusting parameters in the Hamiltonians, these quantum systems may show both integrable and chaotic limits. We provide examples of chaotic systems leading to diffusive and to ballistic transport. In addition, methods of coherent quantum control to induce a transition from diffusive to ballistic transport are proposed.

PACS numbers: 05.30.-d, 05.45.Mt, 05.60.Gg, 03.67.Pp, 75.10.Pq

I. INTRODUCTION

A complete understanding of transport behavior in many-body systems is one of the utmost challenges in fundamental studies of non-equilibrium statistical mechanics. In the classical domain, it is widely believed that chaotic systems should show diffusive (normal) transport, whereas integrability should be associated with ballistic (abnormal) transport [1, 2], although normal transport has also been verified for a non-chaotic system [3]. In the quantum domain, the conditions that determine specific transport behaviors are still under debate, but here also, the main conjecture is of the correspondence integrable-ballistic and chaotic-diffusive [4]. Several theoretical approaches have been undertaken to address this issue, including: attempts to derive the Fourier law from a microscopic foundation by applying the Hilbert space average method [5] and by numerically studying transport of heat in finite chaotic and non-chaotic systems coupled to heat reservoirs [6, 7]; analysis of the transport behavior of local magnetization in isolated finite systems at zero temperature [8]; new advances toward the problem of quantum thermalization [9]; comparisons of the results for conductivity in integrable and chaotic systems at finite temperature and in the thermodynamic limit [10, 11, 12, 13, 14], a subject of intense discussion here being the possibility of ballistic transport in non-integrable quasi-one-dimensional systems [15, 16, 17]; numerical studies of spin diffusion at long times at infinity temperature [18]; as well as studies of transport properties near the metal-insulator transition [19, 20, 21].

Investigations of transport behavior in the particular case of quasi-one-dimensional spin-1/2 systems have been highly motivated by experiments in low-dimensional magnetic compounds, such as copper oxide (cuprate) systems, where ballistic behavior has been observed for heat conduction [22, 23, 24], and also for magnetization, as revealed by nuclear magnetic resonance (NMR) experiments [25]. These compounds are described by models of interacting spins-1/2 arranged in structures such as

chains, two-leg ladders, and square lattices [26]. Clean spin-1/2 Heisenberg chains with only nearest-neighbor interactions are integrable models solved with the Bethe Ansatz method [27], whereas two-dimensional lattices are chaotic [28] and two-leg spin ladder systems become chaotic when the interchain and intrachain interactions are of the same order [29].

In Ref. [8], an isolated isotropic finite spin-1/2 Heisenberg chain at zero temperature and with only nearest-neighbor interactions was considered in the analysis of transport of local magnetization in both cases: when the system was clean and therefore integrable, and when random on-site disorder led to the onset of quantum chaos. Free boundary conditions were assumed. A bouncing behavior of the local magnetization was observed in the integrable regime and interpreted as a hint of ballistic transport, whereas for the chaotic system the local magnetization showed an exponential relaxation to equilibrium, which was considered a reflection of diffusive transport.

The first part of this paper is also dedicated to the investigation of transport of local magnetization in spin-1/2 Heisenberg systems, but different ways to induce chaos are dealt with. The goal is to resolve whether non-integrability may have a unique correspondence with the exponential decay verified in [8]. The integrability-breaking terms considered are: on-site disorder described either by (i) randomly distributed Zeeman energies [30] or by (ii) a few defects placed on specific positions of the chain [31]; and couplings to more surrounding spins such as (iii) next-nearest neighbor interactions and (iv) interchain interactions, as typical of two-leg spin ladder systems. An exponential decay is observed only for (i) and (iv). For the finite systems studied, few defects lead to a behavior that sometimes resembles localization, the exponential behavior appearing only under very special conditions, while next-nearest neighbor interactions generate oscillations of the local magnetization that are similar to those seen for the integrable system, although faster. These observations support the conjecture that chaos might not be a sufficient condition for normal transport.

The second part of this work focuses on the analysis of methods of coherent quantum control, the so-called

*Email: lsantos2@yu.edu

dynamical decoupling (DD) schemes, as potential tools to manipulate transport behavior. DD schemes consist of sequences of external control operations that average out unwanted contributions to the system Hamiltonian. These methods have long been applied in NMR spectroscopy [32, 33], where the goal is to modify the nuclear spin Hamiltonian to eliminate or scale selected internal interactions. More recently, DD has addressed the removal of interactions between the target system and its environment [34] and has been put in a general control-theoretic framework [35]. It has also been considered in studies of transport of information [36]. Here, we introduce DD sequences that suppress the effects of terms leading to quantum chaos, the purpose being the approach to the ballistic transport behavior verified for the integrable system.

The paper is organized as follows. Sec. II explains how the identification of the chaotic regime is performed and describes the models to be considered. Sec. III presents the results for the transport of local magnetization for systems in different regimes. Sec. IV introduces DD sequences to control transport behavior and shows, as an illustration, results for the sequence that cancels the effects of on-site disorder. Concluding remarks are given in Sec. V.

II. QUANTUM CHAOS AND SYSTEM MODEL

A. Signature of Quantum Chaos

For quantum systems, chaos may be identified by analyzing the distribution of spacings s between neighboring energy levels [37, 38]. Quantum levels of integrable systems tend to cluster and are not prohibited from crossing, the typical distribution is Poissonian:

$$P_P(s) = \exp(-s). \quad (1)$$

In contrast, non-integrable systems show levels that are correlated and crossings are strongly resisted, the level statistics is given by the Wigner-Dyson distribution. The exact form of the distribution depends on the symmetry properties of the Hamiltonian. In the case of systems with time reversal invariance it is given by:

$$P_{WD}(s) = \pi s/2 \exp(-\pi s^2/4). \quad (2)$$

To analyze the transition from integrability to chaos, the quantity η , defined as

$$\eta \equiv \frac{\int_0^{s_0} [P(s) - P_{WD}(s)] ds}{\int_0^{s_0} [P_P(s) - P_{WD}(s)] ds}, \quad (3)$$

was introduced in [39], where $s_0 \approx 0.4729$ is the first intersection point of P_P and P_{WD} . For an integrable sys-

tem $\eta \rightarrow 1$, while for a chaotic system $\eta \rightarrow 0$. The critical value below which the system is considered chaotic is chosen to be $\eta = 0.3$ [40].

B. Heisenberg Model

We study homogeneous and isotropic spin-1/2 Heisenberg chains with open boundary conditions, as described by the Hamiltonian:

$$\begin{aligned} H &= H_z + H_{NN} + H_{NNN} \\ &= \sum_{n=1}^L \omega_n S_n^z + \sum_{n=1}^{L-1} J \vec{S}_n \cdot \vec{S}_{n+1} + \sum_{n=1}^{L-2} J' \vec{S}_n \cdot \vec{S}_{n+2}. \end{aligned} \quad (4)$$

Above, \hbar is set equal to 1; $\vec{S}_n = \vec{\sigma}_n/2$ is the spin operator at site n , $\sigma_n^{x,y,z}$ being the Pauli operators; and L corresponds to the number of sites. The parameter ω_n is the Zeeman splitting of spin n as determined by a static magnetic field in the z direction. The system is clean whenever all sites have the same energy splitting $\omega_n = \omega$, and it is disordered when defects characterized by different energy splittings $\omega_n = \omega + d_n$ are present. J and J' are the interaction strengths of nearest-neighbor (NN) and next-nearest-neighbor (NNN) couplings, respectively, and are assumed to be constant.

All calculations in this work are performed in the basis consisting of eigenstates of the total spin operator in the z direction, $S^z = \sum_{n=1}^L S_n^z$. In this basis, the NN and NNN Ising interactions, $S_n^z S_{n+1}^z$ and $S_n^z S_{n+2}^z$, contribute to the diagonal elements of the Hamiltonian, while the XY -terms, $S_n^x S_{n+1}^x + S_n^y S_{n+1}^y$ and $S_n^x S_{n+2}^x + S_n^y S_{n+2}^y$, constitute the off-diagonal elements. The role of the XY -terms is to transfer excitations through the system by exchanging the position of nearest and next-nearest neighboring spins pointing in opposite directions.

Also considered here are two-leg spin ladder systems corresponding to two coupled spin chains as described by

$$\begin{aligned} H &= \sum_{m=1}^2 [H_{z,m} + H_{NN,m}] + H_{1,2} \\ &= \sum_{m=1}^2 \left[\sum_{n=1}^{L/2} \omega_{n,m} S_{n,m}^z + \sum_{n=1}^{L/2-1} J \vec{S}_{n,m} \cdot \vec{S}_{n+1,m} \right] \\ &\quad + \sum_{n=1}^{L/2} J_{\perp} \vec{S}_{n,1} \cdot \vec{S}_{n,2}, \end{aligned} \quad (5)$$

where ω_n and J are as before, m determines the chain in which the site is positioned, and J_{\perp} characterizes the strength of the interchain interaction.

In order to derive meaningful level spacing distributions, before diagonalizing the Hamiltonian and unfolding the spectrum [37, 38], all trivial symmetries of the

system need to be identified. The analysis of symmetries is necessary, because a Poisson distribution may appear whenever Wigner-Dyson distributions from different symmetry sectors are mixed, which may lead to erroneously interpret the system as integrable. In both models considered here, S^z is conserved, therefore, instead of diagonalizing matrices of dimension 2^L , we study the largest subspace. For L even it corresponds to the sector with $S^z = 0$ and dimension $N = \binom{L}{L/2} = L!/[(L/2)!]^2$. Depending on the parameter values, Hamiltonians (4) and (5) may also exhibit the following symmetries [28]: invariance under lattice reflection, which leads to parity conservation; and conservation of total spin $S^2 = (\sum_{n=1}^L \vec{S}_n)^2$, that is $[H, S^2] = 0$ (S^2 symmetry). Notice also that the Heisenberg model with a magnetic field does not commute with the conventional time-reversal operator, however the distribution associated with its chaotic regime is still given by Eq. (2), as discussed in [28, 37].

III. TRANSPORT OF LOCAL MAGNETIZATION

In studies of transport properties, the most popularly used method is the Green-Kubo formula [41]. However, the application of this formula for the treatment of heat transport has been criticized and the use of the Hilbert space average method to demonstrate the emergence of heat diffusion from microscopic models has been suggested as an alternative [5]. This approach has been extended to the analysis of transport of magnetization in Ref. [8].

Here, as in [8], we study the transport of local magnetization as defined by

$$M(t) \equiv \langle \psi(t) | \sum_{n=1}^{L/2} S_{n,m}^z | \psi(t) \rangle. \quad (6)$$

where $|\psi(t)\rangle$ is the state of the system at instant t written in the basis of S^z . The initial states considered come from the sector $S^z = 0$. For system (4), $|\psi(0)\rangle$ has all spins pointing up placed in the first half of the chain, while the remaining down-spins appear in the other half. For the two-leg system, the initial state has all up-spins in one chain and all down-spins in the other. We assume $L = 12$, which leads to $M(0) = 3$ in both cases.

Integrable system. The clean system with only nearest-neighbor interaction, as described by H (4) with $d_n = 0$ and $J' = 0$, corresponds to an integrable model solved with the Bethe Ansatz method [27]. The dynamics for the local magnetization is shown on the left panel at the top of Fig. 1. The bouncing behavior suggests ballistic transport [8]. In what follows, we compare this result with the time evolution of local magnetization for chaotic regimes induced by different ways.

A. Chaos induced by on-site disorder

In the chain with only nearest-neighbor interactions, as given by H (4) with $J' = 0$, chaos may be induced if one or more defects are present.

Random on-site disorder. Assume that the Zeeman energies are given by $\omega_n = \omega + d_n$, where d_n are uncorrelated random numbers with a Gaussian distribution: $\langle d_n \rangle = 0$ and $\langle d_n d_m \rangle = d^2 \delta_{n,m}$ [30]. The transition from integrability ($d = 0$, $\eta \rightarrow 1$), to chaos ($0.05 \lesssim d/J \lesssim 0.7$, $\eta < 0.3$) is indicated by η , which is computed in the sector $S^z = 0$ and is shown on the right panel at the top of Fig. 1. Notice that as $d/J \rightarrow 0$, conservation of parity and total spin start playing a role. At $d/J = 0$, the correct evaluation of η would need to take these symmetries into account [28].

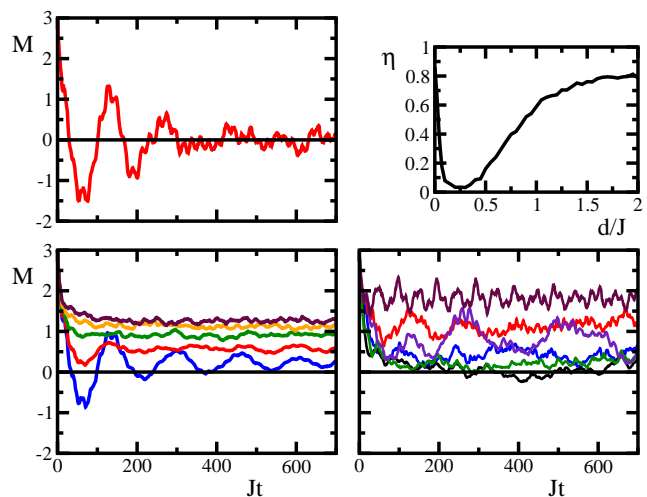


FIG. 1: (Color online.) Transport of local magnetization in a Heisenberg chain with only nearest-neighbor interactions described by H (4) with $J' = 0$ and $L = 12$. The value of ω is irrelevant for the dynamics. Left top panel: $M(t)$ for $d_n = 0$. Right top panel: η computed in the sector $S^z = 0$ for Gaussian random on-site disorder, $\langle d_n \rangle = 0$ and $\langle d_n d_m \rangle = d^2 \delta_{n,m}$. Left bottom panel: $M(t)$ for $d/J = 0.05, 0.1, 0.15, 0.2$, and 0.25 from bottom to top. Average over 20 realizations. Right bottom panel: $M(t)$ for a sample of realizations with $d/J = 0.15$.

On the left panel at the bottom of Fig. 1, we show the time evolution of $M(t)$ averaged over 20 realizations for five different values of d/J in the chaotic region. As we approach chaoticity, for $d/J = 0.05$ and 0.1 , oscillations are still seen; whereas for $d/J = 0.15, 0.2$, and 0.3 , an exponential decay of $M(t)$ takes place reaching final values between 1 and 2. After the decay, the larger probability to find spins pointing up in the first half of the chain is reflected by the positive values of $M(t)$, which are obtained with the majority of the realizations. On the right panel at the bottom, we show the behavior of a sample of realizations with $d/J = 0.15$: for some of them M decays to equilibrium, $M \sim 0$, indicating an equal probability to find up-spins in both halves of the chain, but

for the majority of the realizations $M(t)$ remains positive throughout; hardly any curve reaches negative values of M .

One defect. A single defect in the middle of a chain, at $n = L/2$ (or equivalently at $n = L/2 + 1$), may lead to quantum chaos. For $L = 12$, this happens when $0.15 \lesssim d_6/J \lesssim 2.0$, as discussed in [31]. The transition to chaos is shown by η on the left panel at the top of Fig. 2. The curve is obtained in the $S^z = 0$ sector, but, as mentioned before, for $d_6/J = 0$ the correct evaluation of η would require also the consideration of the S^2 symmetry and parity conservation[28]. A way to break the S^2 symmetry and deal with larger subspaces even when the system is integrable consists of including defects at the edges of the chain [31, 42].

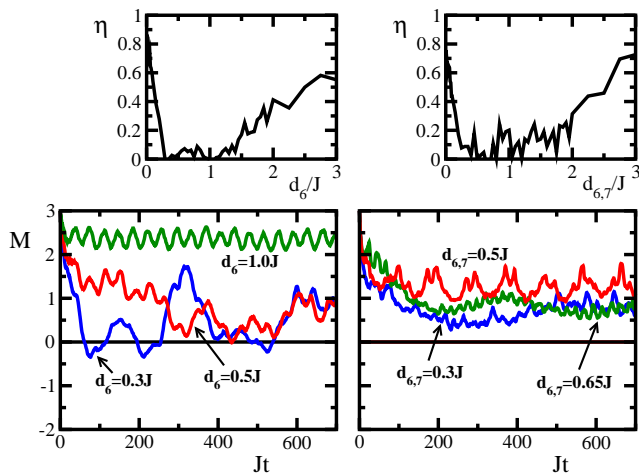


FIG. 2: (Color online.) Transport of local magnetization in a Heisenberg chain with only nearest-neighbor interactions described by $H(4)$ with $J' = 0$ and $L = 12$. Left panels: one defect on site 6, $d_n = 0$ for $n \neq 6$. Right panels: two equal defects on sites 6 and 7, $d_n = 0$ for $n \neq 6, 7$. Top panels: dependence of η on the value of the defect(s). Bottom panels: $M(t)$ for chaotic systems.

The transport of local magnetization is shown on the left panel at the bottom. For $d_6/J = 0.3, 0.5$, and 1.0 , even though η indicates chaoticity, an exponential decay is not observed. Instead, for the two smaller values, especially for the smallest one, partial revivals are verified, whereas for $d_6/J = 1.0$ there occurs localization of the up-spins in the first half of the chain. In contrast, a defect placed on site 7, which shows exactly the same behavior for η , does lead to an exponential decay of $M(t)$ – see right panel of Fig. 3 [43]. The reason for the different results is the following. The initial state $|\uparrow_1\uparrow_2\uparrow_3\uparrow_4 \underbrace{\uparrow_5\uparrow_6}_{\downarrow_8\downarrow_9\downarrow_{10}\downarrow_{11}\downarrow_{12}}\rangle$ is directly coupled only with the state $|\uparrow_1\uparrow_2\uparrow_3\uparrow_4 \underbrace{\uparrow_5\downarrow_6}_{\downarrow_8\downarrow_9\downarrow_{10}\downarrow_{11}\downarrow_{12}}\rangle$. When the defect is on site 6, the hopping of the up-spin from site 6 to site 7 is not favorable, since the state loses the extra energy from the defect site and the positive Ising energy coming from the pair of parallel spins $\uparrow_5\uparrow_6$. This

explains why it becomes easy to localize the initial state by increasing the defect value. Contrary to that, if the defect is on site 7, the Ising energy lost by breaking the pair of parallel spins is regained by placing the up-spin on the defect. In this scenario, directly coupled states may be very close in energy, which favors delocalization.

Two defects. Two equal defects in the middle of the chain, at $n = L/2, L/2 + 1$, may also lead to quantum chaos. For $L = 12$ this happens when $0.15 \lesssim d_{6,7}/J \lesssim 2.0$. The transition to chaos is shown by η on the right panel at the top panel of Fig. 2. The curve is obtained by taking both symmetries into account: conservation of parity and S_z . The relaxation of the local magnetization for $d_{6,7}/J = 0.3, 0.5$ and 0.65 is shown on the right panel at the bottom. The decay is not exponential and $M = 0$ is never reached, most up-spins tending to localize in the first half of the chain. This may again be understood by comparing the energies of the initial state and of the state it is directly coupled to.

The whole spectrum is required to obtain the plots for η presented in Figs. 1 and 2, therefore the decision to deal with relatively small systems, $L = 12$. This choice was a good compromise leading to sufficient statistics and the possibility to run various realizations of random on-site energies. In addition, notice that the behaviors of the local magnetization obtained with $L = 12$ are also reproduced with 10 and 14 spins, as shown in the two panels of Fig. 3. Thus, for the analysis developed in this paper, a system with 12 spins is sufficiently adequate. In order to simulate the time evolution of $M(t)$ in much larger systems, we could resort, for example, to the very efficient algorithm recently proposed in Ref. [44].

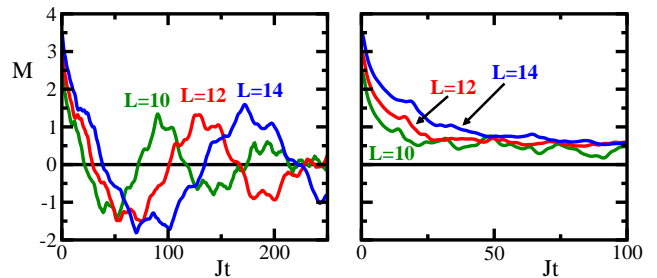


FIG. 3: (Color online.) Transport of local magnetization in a Heisenberg chain of different sizes described by $H(4)$ with $J' = 0$. Left panels: clean chains, $d_n = 0$ for $1 \leq n \leq L$. Right panels: chaotic systems with one defect in site $L/2 + 1$, $d_n = 0$ for $n \neq L/2 + 1$ and $d_{L/2+1}/J = 0.5$.

B. Chaos induced by additional interactions

In a clean Heisenberg system with $d_n = 0$, chaos may be induced by adding frustrating next-nearest neighbor interactions where $J' \sim J$ or by keeping $J' = 0$ and adding interchain interactions where $J_\perp \sim J$ [29]. In both cases, total spin, total spin in the z direction, and parity are conserved.

Next-nearest neighbor interactions. Hamiltonian (4) with $d_n = 0$ and $J = J'$ describes a chaotic system [29]. However, the transport of local magnetization shows oscillations similar to those observed for the integrable system, although at a faster rate, as seen on the left panel of Fig. 4. Therefore, if the bouncing behavior of $M(t)$ in isolated systems at zero temperature is indeed a signature of ballistic transport, integrability is not a necessary condition for abnormal conductivity.

Interchain interaction. Hamiltonian (5) with $d_n = 0$ and $J = J_\perp$ also describes a chaotic system [29]. In this case, as shown on the right panel of Fig. 4, a very fast exponential decay of the local magnetization to equilibrium is indeed verified.

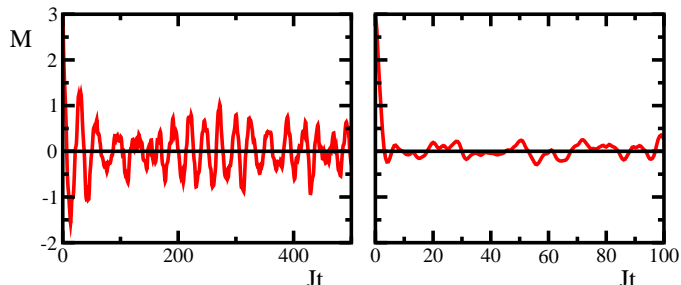


FIG. 4: (Color online.) Transport of local magnetization in a clean Heisenberg system. Left panel: H (4) with $L = 12$, $d_n = 0$, and $J' = J$. Right panel: H (5) with $L = 12$, $d_n = 0$, and $J_\perp = J$.

The distinct behaviors of the transport of local magnetization verified for different chaotic systems – Figs. 1, 2, 3, and 4 – prevent a clear correspondence between chaoticity and diffusive transport. New light may be shed to the problem if this analysis is extended to the transport of other quantities, such as heat in open systems.

IV. CONTROL OF TRANSPORT BEHAVIOR

We propose to control transport behavior by applying DD methods. DD schemes consist of sequences of external control operations that average out unwanted terms of the system Hamiltonian. In the case of spin systems, the control operations correspond to very strong magnetic fields (pulses) able to rotate the spins and time-reverse the system evolution [32, 33]. Here, we assume the ideal scenario, where the pulses are arbitrarily strong and capable of performing instantaneous rotations, the so-called bang-bang controls [34]. Our goal is to eliminate the effects of the terms leading to quantum chaos and approach the transport behavior verified for the integrable system shown Fig. 1. This can be achieved with the sequences described below, where each sequence handles a particular integrability-breaking term.

On-site disorder. The effects of on-site disorder may be eliminated by rotating all spins after every interval of free evolution $t_{j+1} - t_j = \Delta t$, $j \in \mathbb{N}$, by 180° around a di-

rection perpendicular to z , for example x , as determined by the operator,

$$P_x = \exp\left(-i\pi \sum_{n=1}^L S_n^x\right) = \exp(-i\pi S^x).$$

The interaction terms remain undisturbed, but the sequence of these rotations leads to the cancellation of the one-body terms at every $t_{2p} = pT_c$, $p \in \mathbb{N}$, where $T_c = 2\Delta t$ is the cycle time (for details about relevant frames and pulse generation see [45] and references therein). The propagator at a time t_{2p} is then given by

$$U(pT_c) = P_x U(t_{2p}, t_{2p-1}) P_x \dots U(t_2, t_1) P_x U(t_1, 0), \quad (7)$$

where $U(t) = \mathcal{T} \exp[-i \int_0^t H du]$ and \mathcal{T} denotes time ordering. By adopting the notation

$$U_+ = \exp[-i(H_z + H_{NN})\Delta t] = \exp[-iH_1\Delta t],$$

$$\begin{aligned} U_- &= P_x U(t_j, t_{j-1}) P_x = P_x (P_x P_x^\dagger) U(t_j, t_{j-1}) P_x \\ &= -\mathbb{1} \exp\left[-i \left(e^{+i\pi S^x} (H_z + H_{NN}) e^{-i\pi S^x}\right) \Delta t\right] \\ &= -\exp[-i(-H_z + H_{NN})\Delta t] = -\exp[-iH_2\Delta t], \end{aligned}$$

where $\mathbb{1}$ is the identity operator, we rewrite the propagator as

$$U(pT_c) = U_- U_+ \dots U_- U_+ = \exp[-i\bar{H}pT_c].$$

Above, $\bar{H} = \sum_{k=0}^{\infty} \bar{H}^{(k)}$ is the average Hamiltonian [32, 33], and the terms in the sum are obtained by using the Baker-Campbell-Hausdorff expansion. The first two terms are

$$\begin{aligned} \bar{H}^{(0)} &= \frac{\Delta t}{T_c} (H_1 + H_2) = H_{NN}, \\ \bar{H}^{(1)} &= -\frac{i(\Delta t)^2}{2T_c} [H_2, H_1]. \end{aligned}$$

The sequence of pulses reshapes the Hamiltonian. In the ideal limit of $\Delta t \rightarrow 0$ one recovers the Hamiltonian for a clean Heisenberg model with only nearest-neighbor couplings, $\bar{H} \approx H_{NN}$, as desired. In Fig. 5, we show the transport of local magnetization as modified by the above sequence for two cases of on-site disorder: the top panels correspond to random defects and the bottom panels to two defects in the middle of the chain. The transport behavior for both situations – integrable system and disordered Heisenberg chain subjected to the DD sequence – closely coincide when the intervals between the pulses are smaller than the reciprocal interaction strength, $\Delta t < J^{-1}$, as seen on the left panels. For short time evolutions, good agreement between the curves is still verified for $\Delta t \sim J^{-1}$, whereas at longer

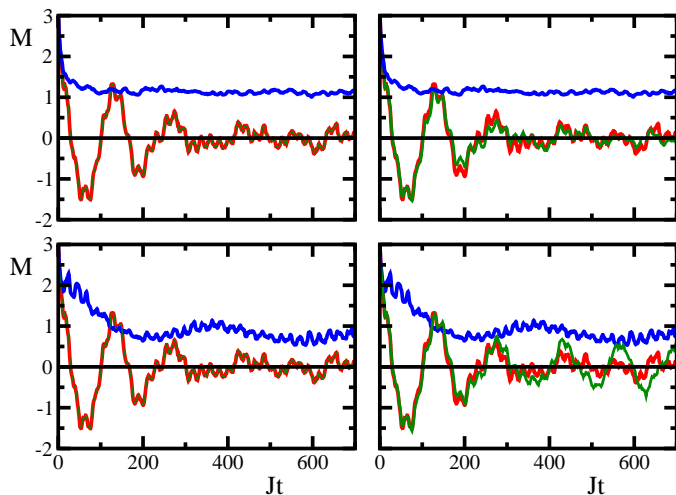


FIG. 5: (Color online.) Transport of local magnetization in a Heisenberg chain with only nearest-neighbor interactions described by H (4) with $J' = 0$ and $L = 12$. (Blue) Curves showing a fast decay to $M(t) \sim 1$ correspond to disordered systems in the absence of pulses. (Green) Bouncing curves represent disordered systems subjected to the DD sequence (7); they closely coincide with the (red) bouncing curves obtained with the clean Heisenberg system. Top panels: Gaussian random on-site disorder, $\langle d_n \rangle = 0$ and $\langle d_n d_m \rangle = d^2 \delta_{n,m}$ with $d/J = 0.2$. Average over 20 realizations. Bottom panels: $d_{6,7}/J = 0.65$ and $d_n = 0$ for $n \neq 6, 7$. Left panels: $\Delta t/J = 0.25$. Right panels: $\Delta t/J = 1.0$. Data is acquired after every $T_c = 2\Delta t$.

times the accumulation of residual averaging errors become significant, this being more perceptible in the bottom right panel. To slow down error accumulation, randomized schemes as developed in [45, 46] may be incorporated to the pulse sequence.

Interchain interactions. To decouple the two interacting chains in a two-leg spin ladder system, we may apply a sequence of π -pulses that rotates all spins of just one of the chains. The pulses do not affect the intrachain interactions, but frequently change the sign of the interchain interactions. To eliminate the interchain couplings in the three directions, we need a sequence of at least four pulses with two alternating directions, such as

$$U(T_c = 4\Delta t) = P_{y,2}U(\Delta t)P_{x,1}U(\Delta t)P_{y,2}U(\Delta t)P_{x,1}U(\Delta t),$$

where

$$P_{x,1} = \exp\left(-i\pi \sum_{n=1}^{L/2} S_{n,1}^x\right),$$

$$P_{y,2} = \exp\left(-i\pi \sum_{n=1}^{L/2} S_{n,2}^y\right).$$

The chain which is subjected to the pulses is also alternated to guarantee the cancellation of the one-body

terms as well. At any time $t_{4p} = pT_c = 4p\Delta t$, we then have $\bar{H} = H_{NN,1} + H_{NN,2} + \mathcal{O}(\Delta t)$.

Next-nearest neighbor interactions. A possible sequence to eliminate next-nearest neighbor interactions involves eight π -pulses. The controls are applied to specifically chosen spins and are only viable if means exist to distinguish them. The suggested pulse sequence is

$$U(T_c = 8\Delta t) = P_8 U(\Delta t) \dots P_2 U(\Delta t) P_1 U(\Delta t),$$

where

$$P_1 = P_3 = \prod_{k=0}^{\lfloor (L-1)/4 \rfloor} e^{-i\pi S_{1+4k}^x} \prod_{k=0}^{\lfloor (L-2)/4 \rfloor} e^{-i\pi S_{2+4k}^x},$$

$$P_2 = P_4 = \prod_{k=0}^{\lfloor (L-3)/4 \rfloor} e^{-i\pi S_{3+4k}^y} \prod_{k=0}^{\lfloor (L-4)/4 \rfloor} e^{-i\pi S_{4+4k}^y},$$

$$P_5 = P_7 = \prod_{k=0}^{\lfloor (L-2)/4 \rfloor} e^{-i\pi S_{2+4k}^x} \prod_{k=0}^{\lfloor (L-3)/4 \rfloor} e^{-i\pi S_{3+4k}^x},$$

$$P_6 = P_8 = \prod_{k=0}^{\lfloor (L-1)/4 \rfloor} e^{-i\pi S_{1+4k}^y} \prod_{k=0}^{\lfloor (L-4)/4 \rfloor} e^{-i\pi S_{4+4k}^y}, \quad (8)$$

At any time $t_{8p} = pT_c = 8p\Delta t$, we obtain $\bar{H} = H_{NN}/2 + \mathcal{O}(\Delta t)$. Apart from a rescaling factor $1/2$, we recover the Hamiltonian for a clean Heisenberg model with only nearest neighbor interactions up to first order in Δt . Notice that the sequence cancels both next-nearest neighbor interactions and one-body terms. The Hamiltonians for the intervals of free evolution are given in the appendix. Since they no longer conserve S_z , simulations involving this pulse sequence need to consider the whole Hilbert space of dimension 2^L .

V. CONCLUSION

The purpose of this work was twofold: to contribute to the ongoing discussion about transport properties of quantum many-body systems and to study the possibility of controlling transport behavior by resorting to dynamical decoupling methods.

Our conclusions are based on the analysis of the transport of local magnetization in isolated finite spin-1/2 systems with free boundary conditions and at zero temperature. Diffusive transport is associated with the exponential decay of the local magnetization and ballistic transport with its bouncing behavior. Under these conditions, it was shown that a one to one correspondence between quantum chaos and normal transport does not necessarily hold; instead, different integrability-breaking terms may lead to both ballistic and diffusive behavior.

Dynamical decoupling sequences capable of suppressing the terms of the Hamiltonian leading to quantum

chaos were proposed. The goal was to approach the ballistic transport behavior of local magnetization obtained with the integrable system. This was achieved by applying pulses separated by intervals smaller than the reciprocal interaction strength, as illustrated for two cases of on-site disorder: random defects and two defects in the middle of the chain.

The manipulation of transport behavior in systems subjected to dynamical decoupling methods is a topic that deserves further exploitation. In particular, the analysis of heat transport in systems coupled to two heat reservoirs at different temperature is one of our future goals. Also important is the identification of real systems where these ideas could be tested experimentally, a

possible good candidate being a crystal of fluorapatite, as proposed in studies of information transport [36].

Acknowledgments

We thank W. G. Brown, G. A. Cwilich, and C. O. Escobar for helpful discussions.

APPENDIX A: SUPPRESSING NEXT-NEAREST NEIGHBOR INTERACTIONS

The pulses from Eq. (8) lead to the propagator

$$\begin{aligned} U(T_c) &= P_8 U(\Delta t) P_7 U(\Delta t) P_6 U(\Delta t) P_5 U(\Delta t) P_4 U(\Delta t) P_3 U(\Delta t) P_2 U(\Delta t) P_1 U(\Delta t) \\ &= \underbrace{(P_8 P_7 \dots P_1)}_{\mathbb{1}} \underbrace{(P_7 \dots P_1)^\dagger U(\Delta t) (P_7 \dots P_1)}_{\exp(-iH_8 \Delta t) \dots \exp(-iH_2 \Delta t)} \dots \underbrace{P_1^\dagger U(\Delta t) P_1}_{\exp(-iH_1 \Delta t)} U(\Delta t) \end{aligned}$$

where, for L even and by using the notation,

$$za = \sum_{k=0}^{\lfloor (L-1)/4 \rfloor} \omega_{1+4k} S_{1+4k}^z \quad zb = \sum_{k=0}^{\lfloor (L-2)/4 \rfloor} \omega_{2+4k} S_{2+4k}^z$$

$$zc = \sum_{k=0}^{\lfloor (L-3)/4 \rfloor} \omega_{3+4k} S_{3+4k}^z \quad zd = \sum_{k=0}^{\lfloor (L-4)/4 \rfloor} \omega_{4+4k} S_{4+4k}^z$$

$$\begin{aligned} X1o &= \sum_{k=1}^{L/2} S_{2k-1}^x S_{2k}^x & X1e &= \sum_{k=1}^{L/2-1} S_{2k}^x S_{2k+1}^x & X2 &= \sum_{n=1}^{L-2} S_n^x S_{n+2}^x \\ Y1o &= \sum_{k=1}^{L/2} S_{2k-1}^y S_{2k}^y & Y1e &= \sum_{k=1}^{L/2-1} S_{2k}^y S_{2k+1}^y & Y2 &= \sum_{n=1}^{L-2} S_n^y S_{n+2}^y \\ Z1o &= \sum_{k=1}^{L/2} S_{2k-1}^z S_{2k}^z & Z1e &= \sum_{k=1}^{L/2-1} S_{2k}^z S_{2k+1}^z & Z2 &= \sum_{n=1}^{L-2} S_n^z S_{n+2}^z \end{aligned}$$

the Hamiltonians during the intervals of free evolutions are

$$\begin{aligned} H_1 &= +za + zb + zc + zd + X1o + X1e + Y1o + Y1e + Z1o + Z1e + X2 + Y2 + Z2 \\ H_2 &= -za - zb + zc + zd + X1o + X1e + Y1o - Y1e + Z1o - Z1e + X2 - Y2 - Z2 \\ H_3 &= -za - zb - zc - zd + X1o - X1e + Y1o - Y1e + Z1o + Z1e - X2 - Y2 + Z2 \\ H_4 &= +za + zb - zc - zd + X1o - X1e + Y1o + Y1e + Z1o - Z1e - X2 + Y2 - Z2 \\ H_5 &= +za + zb + zc + zd + X1o + X1e + Y1o + Y1e + Z1o + Z1e + X2 + Y2 + Z2 \\ H_6 &= +za - zb - zc + zd + X1o + X1e - Y1o + Y1e - Z1o + Z1e + X2 - Y2 - Z2 \end{aligned}$$

$$\begin{aligned}
H_7 &= -za - zb - zc - zd - X1o + X1e - Y1o + Y1e + Z1o + Z1e - X2 - Y2 + Z2 \\
H_8 &= -za + zb + zc - zd - X1o + X1e + Y1o + Y1e - Z1o + Z1e - X2 + Y2 - Z2.
\end{aligned}$$

The sum of these eight intervals lead to the cancellation of the one-body terms and the next-nearest neighbor in-

teraction, so that $\bar{H} = H_{NN}/2 + \mathcal{O}(\Delta t)$.

-
- [1] G. Casati, J. Ford, F. Vivaldi, and W. M. Visscher, *Phys. Rev. Lett.* **52**, 1861 (1984).
- [2] S. Lepri, R. Livi, and A. Politi, *Phys. Rep.* **377**, 1 (2001).
- [3] B. Li, G. Casati, J. Wang, and T. Prosen, *Phys. Rev. Lett.* **92**, 254301 (2004).
- [4] X. Zotos, *J. Phys. Soc. Jpn* **74 Suppl.**, 173 (2005).
- [5] M. Michel, G. Mahler, and J. Gemmer, *Phys. Rev. Lett.* **95**, 180602 (2005); M. Michel, G. Mahler, and J. Gemmer, *Int. J. Mod. Phys. B* **20**, 4855 (2006).
- [6] K. Saito, S. Takesue, and S. Miyashita, *Phys. Rev. E* **54**, 2404 (1996); idem **61**, 2397 (2000).
- [7] C. Mejia-Monasterio, T. Prosen, and G. Casati, *Europhys. Lett.* **72**, 520 (2005); C. Mejia-Monasterio and H. Wichterich, *Eur. Phys. J. Special Topics* **151**, 113 (2007).
- [8] R. Steinigeweg, J. Gemmer, and M. Michel, *Europhys. Lett.* **75**, 406 (2006).
- [9] M. Rigol, V. Dunjko, and M. Olshanii, *Nature* **452**, 854 (2008).
- [10] X. Zotos, F. Naef, and P. Prelovšek, *Phys. Rev. B* **55**, 11029 (1997); X. Zotos, *Phys. Rev. Lett.* **82**, 1764 (1999).
- [11] A. Rosch and N. Andrei, *Phys. Rev. Lett.* **85**, 1092 (2000).
- [12] S. Fujimoto and N. Kawakami, *Phys. Rev. Lett.* **90**, 197202 (2003).
- [13] P. Jung, R. Helmes, and A. Rosch, *Phys. Rev. Lett.* **96**, 067202 (2006).
- [14] F. Heidrich-Meisner, A. Honecker, and W. Brenig, *Eur. Phys. J. Special Topics* **151**, 135 (2007).
- [15] J. V. Alvarez and C. Gros, *Phys. Rev. Lett.* **89**, 156603 (2002).
- [16] F. Heidrich-Meisner, A. Honecker, D. C. Cabra, and W. Brenig, *Phys. Rev. Lett.* **92**, 069703 (2004).
- [17] X. Zotos, *Phys. Rev. Lett.* **92**, 067202 (2004).
- [18] K. Fabricius and B. M. McCoy, *Phys. Rev. B* **57**, 8340 (1998).
- [19] B. Kramer and A. MacKinnon, *Rep. Prog. Phys.* **56**, 1469 (1993).
- [20] G. M. G. Bouzerar, D. Poilblanc, *Phys. Rev. B* **49**, 8258 (1994).
- [21] D. M. Basko, I. L. Aleiner, and B. L. Altshuler, *Ann. Phys.* **321**, 1126 (2006); D. M. Basko, I. L. Aleiner, and B. L. Altshuler, arXiv:cond-mat/0602510.
- [22] K. Kudo, S. Ishikawa, T. Noji, T. Adachi, Y. Koike, K. Maki, S. Tsuji, and K. Kumagai, *J. Low Temp. Phys.* **117**, 1689 (1999).
- [23] A. V. Sologubenko, K. Giannò, H. R. Ott, U. Ammerahl and A. Revcolevschi, *Phys. Rev. Lett.* **84**, 2714 (2000); A. V. Sologubenko, K. Giannò, H. R. Ott, A. Vietkine, and A. Revcolevschi, *Phys. Rev. B* **64**, 054412 (2001).
- [24] C. Hess, C. Baumann, U. Ammerahl, B. Büchner, F. Heidrich-Meisner, W. Brenig, and A. Revcolevschi, *Phys. Rev. B* **64**, 184305 (2001); C. Hess, B. Büchner, U. Ammerahl, L. Colonescu, F. Heidrich-Meisner, W. Brenig, and A. Revcolevschi, *Phys. Rev. Lett.* **90**, 197002 (2003).
- [25] M. Takigawa, N. Motoyama, H. Eisaki, and S. Uchida, *Phys. Rev. Lett.* **76**, 4612 (1996).
- [26] C. Hess, *Eur. Phys. J. Special Topics* **151**, 73 (2007).
- [27] H. A. Bethe, *Z. Phys.* **71**, 205 (1931); M. Karbach and G. Müller, *Comput. Phys.* **11**, 36 (1997).
- [28] W. G. Brown, L. F. Santos, D. Starling, and L. Viola, *Phys. Rev. E* **77**, 021106 (2008).
- [29] T. C. Hsu and J. C. A. d'Auriac, *Phys. Rev. B* **47**, 14291 (1993).
- [30] Y. Avishai, J. Richert, and R. Berkovitz, *Phys. Rev. B* **66**, 052416 (2002).
- [31] L. F. Santos, *J. Phys. A* **37**, 4723 (2004).
- [32] U. Haeberlen, *High Resolution NMR in Solids: Selective Averaging* (Academic Press, New York, 1976).
- [33] R. R. Ernst, G. Bodenhausen, and A. Wokaun, *Principles of Nuclear Magnetic Resonance in One and Two Dimensions* (Oxford University Press, Oxford, 1994).
- [34] L. Viola and S. Lloyd, *Phys. Rev. A* **58**, 2733 (1998).
- [35] L. Viola, E. Knill, and S. Lloyd, *Phys. Rev. Lett.* **82**, 2417 (1999); idem **83**, 4888 (1999).
- [36] P. Cappellaro, C. Ramanathan, and D. G. Cory, *Phys. Rev. Lett.* **99**, 250506 (2007); P. Cappellaro, C. Ramanathan, and D. G. Cory, *Phys. Rev. A* **76**, 032317 (2007).
- [37] F. Haake, *Quantum Signatures of Chaos* (Springer-Verlag, Berlin, 1991).
- [38] T. Guhr, A. Mueller-Gröeling, and H. A. Weidenmüller, *Phys. Rep.* **299**, 189 (1998).
- [39] P. Jacquod and D. L. Shepelyansky, *Phys. Rev. Lett.* **79**, 1837 (1997).
- [40] B. Georgeot and D. L. Shepelyansky, *Phys. Rev. E* **62**, 3504 (2000).
- [41] R. Kubo, M. Toda, and N. Hashitsume, *Statistical Physics II: Nonequilibrium Statistical Mechanics*, (Springer, 2nd Ed., Berlin, Heidelberg, New-York, 1991).
- [42] L. F. Santos, G. Rigolin, and C. O. Escobar, *Phys. Rev. A* **69**, 042304 (2004).
- [43] The different behaviors of $M(t)$ associated with the position of the defect was mentioned to us by R. Steinigeweg in private communication.
- [44] M. B. Hastings, *Phys. Rev. B* **77**, 144302 (2008).
- [45] L. F. Santos and L. Viola, *New J. Phys.* **10**, 083009 (2008).
- [46] L. Viola and E. Knill, *Phys. Rev. Lett.* **94**, 060502 (2005); L. F. Santos and L. Viola, *Phys. Rev. A* **72**, 062303 (2005); O. Kern and G. Alber, *Phys. Rev. Lett.* **95**, 250501 (2005); L. F. Santos and L. Viola, *Phys. Rev. Lett.* **97**, 150501 (2006).